

Performance Enhancement of Hybrid Renewable Energy System for AC Microgrid

Mohamed Selmy
Department of Electrical
Engineering, Faculty of
Engineering at Shoubra, Benha
University, Cairo, Egypt
mohamed.selmy@feng.bu.edu.eg

H. A. AbdelHadi
Department of Electrical
Engineering, Faculty of
Engineering at, Shoubra, Benha
University, Cairo, Egypt
hosam.abdelhady@feng.bu.edu.eg

Ahmed Abdulnabi
Department of Electrical
Engineering, Faculty of
Engineering at, Shoubra, Benha
University, Cairo, Egypt
ahmed.abdelnabee@feng.bu.edu.eg

E. M. Saied
Department of Electrical
Engineering, Higher
Technological of Institute 10th of
Ramadan, City, Egypt
On leave: Faculty of Engineering
at Shoubra, Benha University,
Cairo, Egypt
ebtisam.saied@feng.bu.edu.eg

Abstract— The rapid increase in the depending on green energy sources to deliver power, especially to remote areas poses a challenging task for engineers to regulate and obtain the most power available from these sources. This study focuses on problems with power changes caused by the impacts of wind and/or solar variations that are related to weather conditions. Variable voltage and output power result from these effects because they limit the ability to use various power sources. Controller design and metaheuristic optimization methods such as the honey badger algorithm (HBA) and particle swarm optimization (PSO) are presented to overcome these issues. There have been investigations into the design and identification of the hybrid power microgrid system components. MATLAB/Simulink is used to simulate, control, and model the system. The obtained results show how optimized controllers using the HBA technique compared to PSO are more effective with efficiency reaching 99.9% of maximum power generation and total harmonic distortion (THD) reaching 1.99%.

Keywords— Hybrid Power System, Wind Energy, Photovoltaic Cell, Battery, Particle Swarm Optimization, Honey Badger Algorithm

I. INTRODUCTION

In areas that are difficult to reach by grid connection systems, renewable energy sources (RES) are employed to supply electrical energy and give a solution to the issue of energy deficits [1], [2]. Due to environmental issues, microgrids (MGs) are a major component in future power systems [3]. According to the MGs' definition, they are regional distribution networks that can generate, store, and carry loads. They can operate independently or in connection with the main grid. A standalone hybrid renewable energy system combines at least one renewable energy source, but it is not connected to the grid. The configuration of RES in power generation systems begins with the residential system and progresses to a microgrid system [4]. It can perform both when connected to and an isolated from the main grid, enhancing the stability and quality of the electricity sent to the connected customers [5]. MGs are classified based on their size, type, scenario, and mode of operation. MGs consist of loads, a controller, a point of common coupling, distributed generation such as solar, wind, fuel cells, and microturbines, intermediate storage such as superconducting magnetic and compressed air energy storage, flywheels, and batteries [6]-[16].

The following are the paper's main contributions: First, the use of an enhanced maximum power point tracking (MPPT) method based on the incremental conductance (IC) method with an optimized proportional-integral (PI) controller using PSO and HBA for photovoltaic systems as well as using the is the perturb and observe (P&O) method with a variable perturbation step method for wind system to allow maximum power point (MPP) tracking even with changing weather conditions; second, controlling the battery bank's charging and discharging operations; and finally, obtaining the desired output voltage and frequency for AC loads.

The remaining part of this paper is divided into the following sections: Section 2 presents a dynamic description and design of the system. The system model is created in section 3. In Section 4, the optimized controller is described. The system's performance is displayed for various weather conditions in Section 5. The work is concluded in Section 6.

II. SYSTEM DESCRIPTION AND DESIGN

As shown in Fig. 1, the planned hybrid renewable energy system (HRES) contains three subsystems: a photovoltaic subsystem, a wind energy subsystem, and a battery bank subsystem. As seen in Fig. 1, a voltage source inverter (VSI) is used to connect the HRES subsystems to the AC loads. The proposed system's components are shown in Table I, which are chosen to match the AC loads.

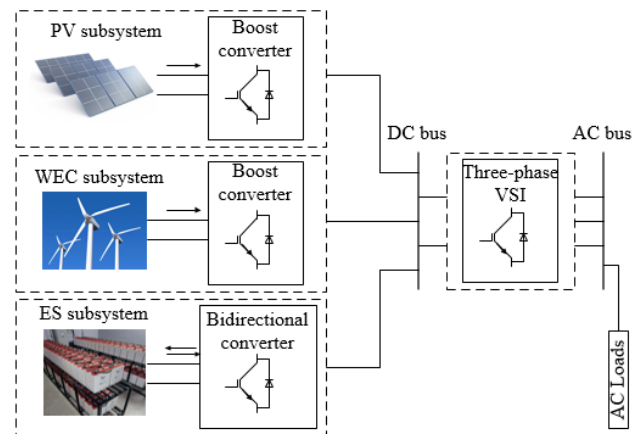


Fig. 1. The overall proposed system

TABLE I. THE PARAMETERS OF THE SYSTEM

Subsystem	Parameter's Specifications
PV subsystem	The 6-kW PV array uses 30 KC200GT PV modules.
Wind subsystem	WT output power is 20 kW at 12 m/s wind speed.
Battery bank subsystem	Voltage is 216 V, and Ampere hour rating is 150.
DC-DC boost converter for the PV subsystem	The frequency of switching is 5 kHz, the filter inductor is 20 mH, and the filter capacitor is 3000 μ F.
DC-DC boost converter for the wind subsystem	The frequency of switching is 5 kHz, the filter inductor is 5 mH, and the filter capacitor is 3000 μ F.
Bidirectional converter for battery subsystem	Filter inductor is 5 mH, and Filter capacitor is 220 μ F.
Two-level converter	DC voltage is 620 V, AC voltage per phase is 220 V, and Frequency is 50 Hz.
LC filter	The filter inductor is 6 mH, and the filter capacitor is 500 μ F.
AC loads	Phase voltage is 220 V and Frequency is 50 Hz. Active power of load (1) is 5 kW, load (2) is 4 kW and 0.5 kvar, and load (3) is 9 kW and 3 kvar.

A. Model of the PV Subsystem

There are different electrical mathematical models are employed for each PV cell. The single-diode model is used because it is widely available, as shown in Fig. 2. It is given by the below equations [17].

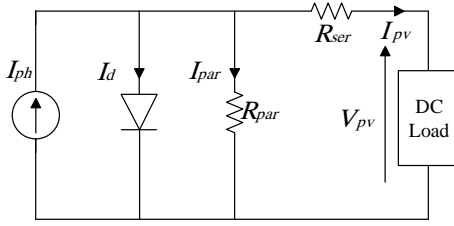


Fig. 2. Equivalent circuit of the PV cell

$$I_{pv} = I_{ph} - I_d - I_{par} \quad (1)$$

Where,

- I_{pv} : the PV cell's output current, A
- I_{ph} : the photocurrent produced by the incident light, A
- I_d : the current of the diode, A
- I_{par} : the shunt resistance current, A.

$$I_d = I_o \left(\exp \left(\frac{V_{pv} + I_{pv} R_{ser}}{\alpha V_t} \right) - 1 \right) \quad (2)$$

$$V_t = \frac{kT}{q} \quad (3)$$

Where,

- I_o : the leakage current of the diode, A
- V_t : the PV cell's terminal voltage, V
- R_{ser} : the PV cell's series resistance, Ω
- V_t : the thermal voltage, V
- α : diode quality factor.

$$I_{par} = \frac{V_{pv} + I_{pv} R_{ser}}{R_{par}} \quad (4)$$

Where,

R_{par} : the PV cell's parallel resistance, Ω .

By substituting (2) and (3) in (1), then

$$I_{pv} = I_{ph} - I_o \left(\exp \left(\frac{V_{pv} + I_{pv} R_{ser}}{\alpha V_t} \right) - 1 \right) - \frac{V_{pv} + I_{pv} R_{ser}}{R_{par}} \quad (5)$$

Utilizing the Newton-Raphson approach, the PV module's undefined values are determined [18], which is shown in Table II, for the selected PV subsystem.

TABLE II. UNKNOWN PARAMETERS

I_{ph} (A)	I_o (A)	R_p (Ω)	R_s (Ω)	α
8.200	1.5454e-07	601.7013	0.2207	1.3336

The variation in solar intensity and temperature impacts the PV system. Table III shows the PV module's specifications [19].

TABLE III. THE ELECTRICAL SPECIFICATIONS OF MODEL KC200GT

Maximum Power	200W (+10% / -5%)
Voltage at Max. Power	26.3V
Current at Max. Power	7.61A
Open Circuit Voltage	32.9V
Short Circuit Current	8.21A

Figs. 3 and Fig. 4 show the electrical characteristics of the PV module when the solar intensity is varied, which are compared with those provided in the KC200GT PV module datasheet.

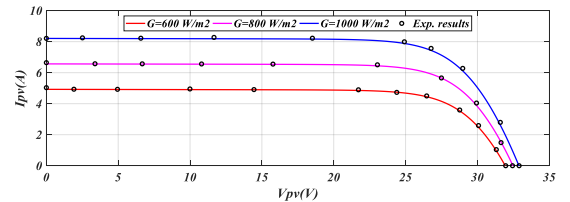


Fig. 3. I-V characteristics at standard T and varying G

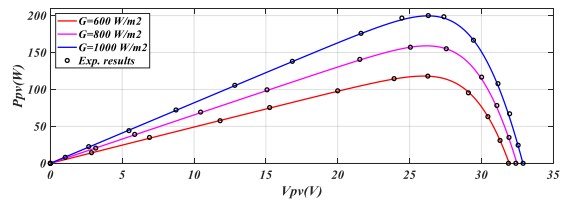


Fig. 4. P-V characteristics at standard T and varying G

In the PV subsystem illustrated in Fig. 5, a boost converter with the MPPT algorithm is used to obtain the most power in accordance with cell temperature and irradiance [20].

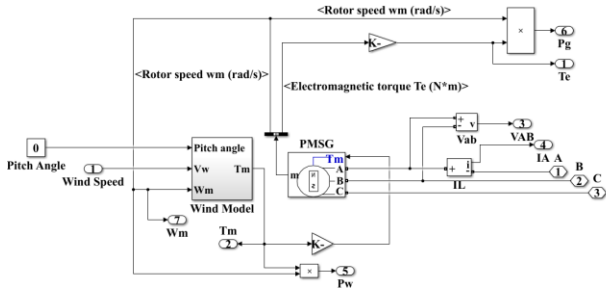


Fig. 12. The WT with PMSG block diagram

C. Model of the Battery Subsystem

When the use of a battery, wind energy and PV systems should be integrated with a common DC link of a certain voltage. This link is used for all power transfers, whether they be from the battery to the load, from the RES to the load, or from RES to the battery. So, a DC/DC bidirectional converter is required to control the DC link voltage as well as charge and/or discharge the battery in the instance of an extra and/or unavailability of power, respectively. The battery subsystem block diagram is illustrated in Fig. 13.

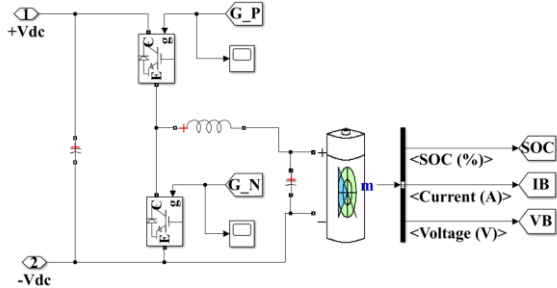


Fig. 13. The battery model

III. SYSTEM CONTROL DESIGN

In this section, there are four main controllers: The first controller is the incremental conductance with an optimized PI controller method to obtain the highest power available from the PV system during different solar intensities, which is shown in Fig. 14. The second controller is the perturb and observe method with a variable perturbation step to generate the greatest power available from a WT under varying wind speed, as shown in Fig. 15. The third controller is an optimized PI controller that is used in the bidirectional converter to allow the battery system is to use the energy that is stored during times of normal operation when wind or solar PV energy is not available, as shown in Fig. 16. The fourth controller is the SVPWM with optimized PI controller used in VSI to produce smooth AC voltages with a fixed frequency, which is shown in Fig. 17. The gains of PI controllers are optimized using PSO and HBA algorithms and their obtained values are given in Table IV. The pseudo codes of PSO and HBA techniques are illustrated in algorithms I and II respectively.

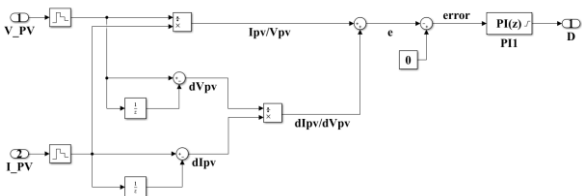


Fig. 14. The IC method based on the PI block diagram

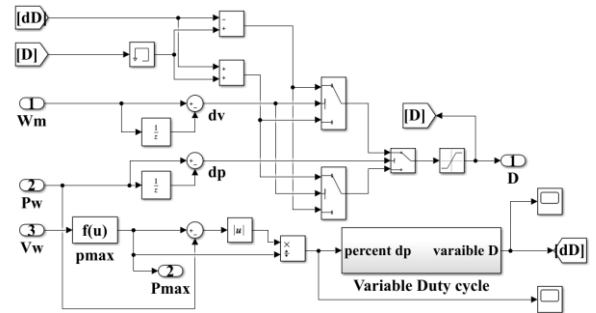


Fig. 15. The P&O method with variable step size block diagram

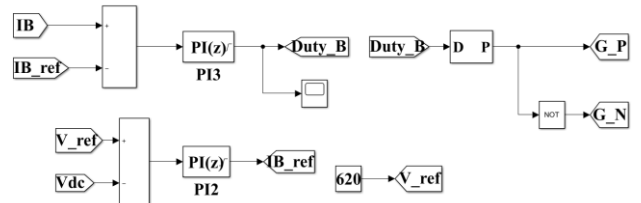


Fig. 16. The bidirectional control block diagram based on PI

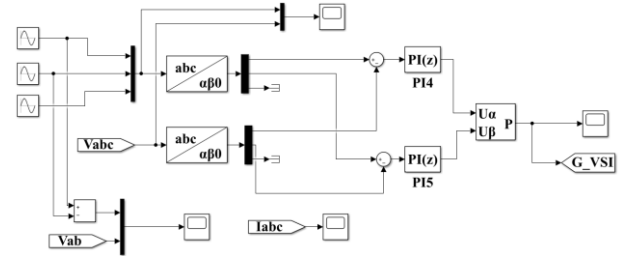


Fig. 17. The SVPWM control block diagram based on PI

TABLE IV. GAINS OF OPTIMIZED PI'S

No.	PSO	HBA
PI (1)	Kp=70.3591 Ki=96.1838	Kp=93.0255 Ki=0.0105
PI (2)	Kp=13.9164 Ki=25.9946	Kp=2.71905 Ki=0.0106
PI (3)	Kp=25.7831 Ki=24.8618	Kp=86.542 Ki=0.0104
PI (4)	Kp=35.1047 Ki=25.4300	Kp=50.012 Ki=0.0105
PI (5)	Kp=47.4732 Ki=83.3415	Kp=24.7927 Ki=73.2428

Algorithm I Pseudo code of PSO

```

for each particle
    Initialize position and velocity randomly
t=1
do
    for each particle
        Calculate fitness function
        if fitness value > pBest Then
            Set current fitness value as pBest
    Update particle with best fitness value as gBest
    for each particle
        Calculate new velocity
        Update position
    t=t+1
while (t < maximum iterations)
Post process the result.

```

Algorithm II Pseudo code of HBA

```

Set parameters  $t_{max}$ ,  $N$ ,  $\beta$ ,  $C$ .
Initialize population with random positions.
Evaluate each honey badger position  $x_i$  fitness using cost function and assign to  $f_i$ ,  $i \in [1, 2, \dots, N]$ .
Save best position  $x_{prey}$  and accredit fitness to  $f_{prey}$ .
while  $t \leq t_{max}$  do
  Update decreasing factor  $\alpha$ 
  for  $i = 1$  to  $N$  do
    Calculate intensity  $I_i$ 
    if  $r < 0.5$  then
      Update position  $x_{new}$  in digging phase
    else
      Update position  $x_{new}$  in honey phase
    end if
    Evaluate new position and assign to  $f_{new}$ 
    if  $f_{new} \leq f_i$  then
      Set  $x_i = x_{new}$  and  $f_i = f_{new}$ 
    end if
    if  $f_{new} \leq f_{prey}$  then
      Set  $x_{prey} = x_{new}$  and  $f_{prey} = f_{new}$ 
    end if
  end for
end while Stop criteria satisfied
Return  $x_{prey}$ 

```

IV. SIMULATION RESULTS AND DISCUSSION

The variables in the AC microgrid system are studied in relation to variable solar radiation and wind speed, such as the AC voltage, AC current, and load power. Fig. 18 illustrates the AC load voltage during this change and variable AC loads, and the AC load current is also illustrated in Fig. 19. Fig. 20 shows the transmitted power from HRES to the AC loads when the irradiance level is changed, and wind speed also is changed.

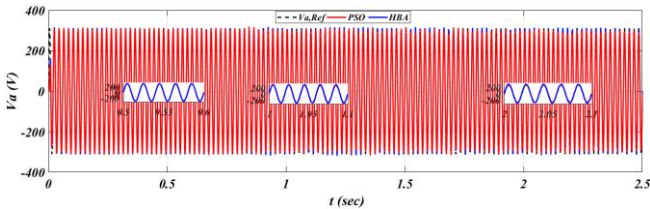


Fig. 18. AC voltage with the hybrid renewable energy system

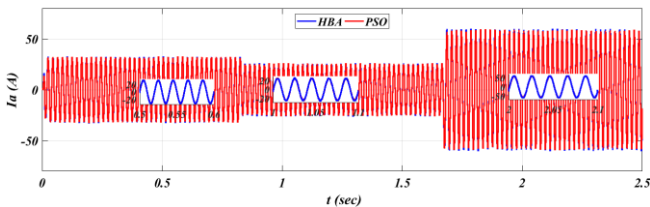


Fig. 19. AC current with the hybrid renewable energy system

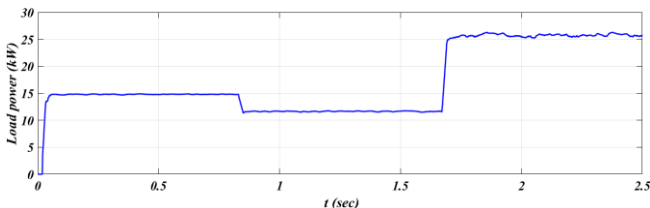


Fig. 20. Transmitted power into the AC loads

The PV output power for the IC technique with an optimized PI controller under varying solar intensity and a nominal cell temperature is shown in Fig. 21.

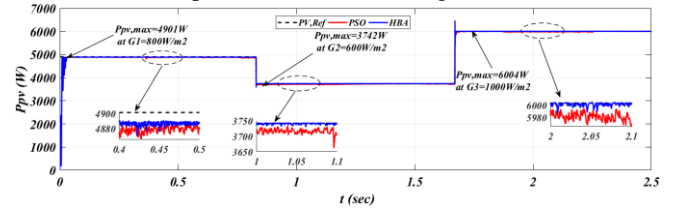


Fig. 21. PV power using the IC method with optimized PI

Obtained maximum PV power is improved using HBA (99.9%) compared to PSO (99.5%), as given in Table V. Fig. 22 shows the AC output voltage while the DC input voltage of the inverter is shown in Fig. 23. From Table VI, the THD of the AC output voltage is reduced by using the HBA (1.99%) optimization technique compared to the PSO (3.06%). Fig. 24 displays the WT's output power in various wind conditions.

TABLE V. SIMULATION RESULTS OF THE IC ALGORITHMS

ΔG (W/m ²)	IC algorithm	P_{pv} (W)	ΔP_{pv} (W)	(%TF)
0:800	Optimized PI- PSO	4874	23	99.45
0:800	Optimized PI- HBA	4889	12	99.76
800:600	Optimized PI- PSO	3715	27	99.28
800:660	Optimized PI- HBA	3741	1	99.97
600:1000	Optimized PI- PSO	5984	20	99.67
600:1000	Optimized PI- HBA	6003	1	99.98

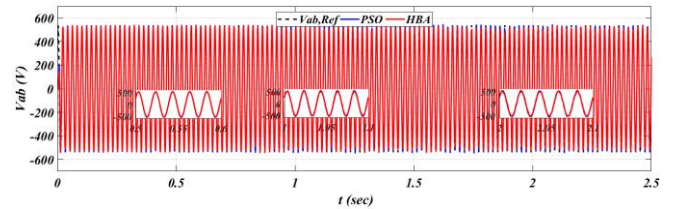


Fig. 22. The AC output voltage of the inverter

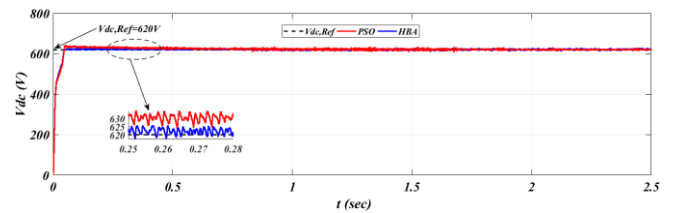


Fig. 23. The DC input voltage of the inverter

TABLE VI. SIMULATION RESULTS OF THE SVPWM

Load	SVPWM with optimized PI	V_{ab} (V) at 50Hz	ΔV_{ab} (V)	(%THD)
Load (1)	PSO	529.8	7.6	1.75%
	HBA	536.3	1.1	1.06%
Load (2)	PSO	519	18.4	3.97%
	HBA	532.4	5	2.39%
Load (3)	PSO	517.8	19.6	3.46%
	HBA	529.5	7.9	2.54%

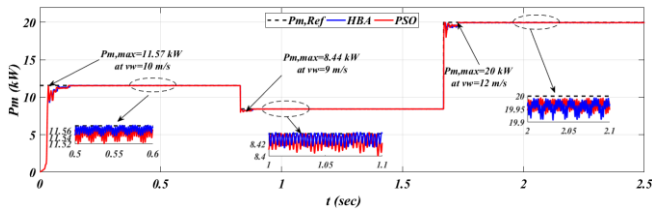


Fig. 24. Turbine output power at different wind speed

V. CONCLUSION

A hybrid photovoltaic, wind, and battery system for AC microgrid is modelled and controlled. The maximum power, under different irradiance values and varying wind speeds, is obtained by optimized PI controllers using PSO and HBA techniques. The simulated system shows promising results using HBA compared to PSO in terms of output power efficiency reached 99.9% and THD in output AC voltage reached 1.99%. The author expected to obtain more promising results if a hybrid PSO-HBA algorithm is used.

REFERENCES

- [1] A. Mohamed, M. E. Bahgat, and A. -G. M. Abdel-Ghany, "Robust Control of Isolated Microgrid based on Decentralized Fixed Structure H_{∞} Loop Shaping," 22nd International Middle East Power Systems Conference (MEPCON), 2021, pp. 575-580.
- [2] F. Anam, A. A. Sahito, and A. Shah, "Comparison of AC and DC Microgrid Considering Solar-Wind Hybrid Renewable," Engineering Science and Technology International Research Journal (ESTIRJ), vol. 4, no. 1, 2018, pp. 33-38.
- [3] S. M. Kaviri, M. Pahlevani, P. Jain, and A. Bakhshai, "A review of AC microgrid control methods," 2017 IEEE 8th International Symposium on Power Electronics for Distributed Generation Systems (PEDG), 2017, pp. 1-8.
- [4] H. K. Khalil, S. M. Yousri, and N. H. El-Amari, "Smart Energy Management for Multi-Microgrid," 2021 22nd International Middle East Power Systems Conference (MEPCON), 2021, pp. 548-555.
- [5] R. Karthik, A. S. Hari, Y. V. Pavan Kumar, and D. J. Pradeep, "Modelling and Control Design for Variable Speed Wind Turbine Energy System," 2020 International Conference on Artificial Intelligence and Signal Processing (AISP), 2020, pp. 1-6.
- [6] F. A. Hashim, E. H. Houssein, K. Hussain, M. S. Mabrouk, and W. Al-Atabany, "Honey Badger Algorithm: New metaheuristic algorithm for solving optimization problems," Math. Comput. Simul., vol. 192, 2022, pp. 84-110.
- [7] A. M. Ewais, R. El-Azab and M. A. A. Adma, "Stand-Alone Microgrid Energy Storage Schemes: Comparative Study," 2018 Twentieth International Middle East Power Systems Conference (MEPCON), 2018, pp. 564-569.
- [8] K. H. Ahmed, S. J. Finney, and B. W. Williams, "Passive filter design for three-phase inverter interfacing in distributed generation," 5th Int. Conf. Comput. Power Electron. CPE 2007, 2007, pp. 1-9.
- [9] V. Salas, W. Suponthana, and R. A. Salas, "Overview of the off-grid photovoltaic diesel batteries systems with AC loads," Appl. Energy, vol. 157, 2015, pp. 195-216.
- [10] M. Kishan, P. S. Arun, K. V. Kumar, A. Michael, J. P. John, and S. Suresh Kumar, "Simulation And Comparison Of Spwm And Svpwm Control For Three Phase Inverter Related Papers Modified Pwm Control Met Hods Of Z Source Invert Er For Drive Applicat Ions Simulation And Comparison Of Spwm And Svpwm Control For Three Phase Inverter," vol. 5, no. 7, 2010, pp. 1819-6608, [Online]. Available: www.arpnjournals.com.
- [11] H. S. Das, A. Dey, T. C. Wei, and A. H. M. Yatim, "Feasibility analysis of standalone PV/wind/battery hybrid energy system for rural Bangladesh," Int. J. Renew. Energy Res., vol. 6, no. 2, 2016, pp. 402-412.
- [12] K. M. Kotb, M. F. Elmorshedy, H. S. Salama, and A. Dán, "Enriching the stability of solar/wind DC microgrids using battery and superconducting magnetic energy storage based fuzzy logic control," J. Energy Storage, vol. 45, 2022, pp. 103-751.
- [13] O. A. Mosaad Ali, H. M. El-Zoghby and A. G. M. A. Ghany, "Maximum Power Point Tracking for Hybrid Wind-Solar Energy System Using Optimum Controllers Techniques," 2018 Twentieth International Middle East Power Systems Conference (MEPCON), 2018, pp. 504-509.
- [14] D. V. Samokhvalov, A. I. Jaber, D. M. Filippov, A. N. Kazak and M. S. Hasan, "Research of Maximum Power Point Tracking Control for Wind Generator," 2020 IEEE Conference of Russian Young Researchers in Electrical and Electronic Engineering (EIConRus), 2020, pp. 1301-1305.
- [15] M. A. Ebrahim, H. A. Abdelhadi, H. M. Mahmoud, E. M. Saied, and M. M. Salama, "Optimal Design of MPPT Controllers for Grid Connected Photovoltaic Array System," Int. J. Emerg. Electr. Power Syst., vol. 17, no. 5, 2016, pp. 511-517.
- [16] M. A. Ebrahim, B. A. Aziz, F. A. Osman and M. N. F. Nashed, "Optimal PI Based Secondary Control for Autonomous Micro-Grid via Particle Swarm Optimization Technique," 2018 Twentieth International Middle East Power Systems Conference (MEPCON), 2018, pp. 1148-1155.
- [17] H. A. Mohamed, H. A. Khattab, A. Mobarka and G. A. Morsy, "Design, control and performance analysis of DC-DC boost converter for stand-alone PV system," 2016 Eighteenth International Middle East Power Systems Conference (MEPCON), 2016, pp. 101-106.
- [18] A. Hussein, "A simple approach to extract the unknown parameters of PV modules," Turkish Journal of Electrical Engineering & Computer Sciences, 2017, pp. 4431-4444.
- [19] KC200GT High Efficiency Multicrystal Photovoltaic Module Kyocera. <http://www.kyocera.com.sg/products/solar/pdf/kc200gt.pdf>.
- [20] X. Zhou, D. Song, Y. Ma, and D. Cheng, "The simulation and design for MPPT of PV system based on incremental conductance method," in Proceedings - 2010 WASE International Conference on Information Engineering, ICIE 2010, vol. 2, 2010, pp. 314-317.
- [21] I. M. Abdelqawee, A. Y. Yousef, K. M. Hasaneen, M. N. F. Nashed, and H. G. Hamed, "Standalone wind energy conversion system control using new maximum power point tracking technique," Int J Emerg Technol Adv Eng Certif J, vol. 9, no. 2, 2019, pp. 95-100.
- [22] Catalogue of European Urban Wind Turbine Manufacturers, Page 27. Available at: http://www.urbanwind.net/pdf/CATALOGUE_V2.pdf.